ELSEVIER

Journal of Power Sources 72 (1998) 83–90

JOURNAL OF POWER SOURCES

A study of the electrochemical lithium intercalation behavior of porous $LiNiO_2$ electrodes prepared by solid-state reaction and sol–gel methods

Young-Min Choi [a], Su-Il Pyun [a,*], Seong-In Moon [b], Yoo-Eup Hyung [b]

[a] *Department of Materials Science and Engineering, Korea Advanced Institute of Science and Technology, 373-1 Kusung-Dong, Yusong-Gu, Daejon 305-701, South Korea*

[b] *Battery Technology Team, Korea Electrotechnology Research Institute, 28-1 Sungju-Dong, Changwon 641-600, South Korea*

Received 5 May 1997; accepted 9 June 1997

Abstract

The electrochemical lithium intercalation behavior of porous $LiNiO_2$ electrodes prepared by solid-state reaction and sol–gel methods is investigated by using X-ray diffractometry (XRD), a galvanostatic intermittent charge–discharge experiment, electrochemical impedance spectroscopy(EIS), and a charge–discharge cycling test. The ultrafine $LiNiO_2$ powder is prepared by the sol–gel method in order to overcome the disadvantage of the conventional solid-state reaction method. From the results of XRD, the layered $LiNiO_2$ phase proves to be stable above 400°C. The conventional oxide electrode suffers a larger capacity loss, a greater instantaneous IR drop during the first intermittent discharge, and a smaller chemical diffusivity than the gel-derived electrode. The results are discussed with respect to the marked cation mixing effect in the former electrode. Furthermore, the charge–discharge cycling test shows that the cell Li/organic electrolyte/gel-derived $LiNiO_2$ electrode displays improved performance, i.e., an initial specific capacity of 150 Ah kg^{-1} and a specific energy density above 500 Wh kg^{-1}.

Keywords: $LiNiO_2$; Sol–gel method; Electrochemical lithium intercalation; Chemical diffusivity; Cation mixing

1. Introduction

Rechargeable lithium batteries, because of their higher energy density, higher voltage, and longer shelf-life than competitive system like Ni–metal hydride battery, have attracted much attention over the last decade [1–3]. Recently, 'rocking-chair' or 'lithium ion' battery technology was developed to overcome the reversibility and safety problems associated with the lithium metal anode [4]. In this technology, lithium is confined to its ionic state, which is inherently safer than its metallic state. In order to compensate the loss in the cell potential at carbon anode compared with lithium metal, a strongly oxidizing intercalation compound must be used as a cathode material [5]. Among these cathode materials, $LiNiO_2$ [6,7] and $LiCoO_2$ [8,9] have been intensively studied due to their very promising electrochemical performances. Although the former has good reversibility, it is difficult to synthesize unless the proper processing methods are applied. Nevertheless, much attention has been recently paid to $LiNiO_2$ due to its low cost and good charge retention compared with the first commercial material $LiCoO_2$ [10].

Several solution methods have been developed to circumvent the problems of the solid-state reaction method and enhance the physicochemical and electrochemical properties of the transition metal oxide powder systems [11–13].

There have been few reports, however, of the synthesis of $LiNiO_2$ powder by the solution method. The sol–gel method, one of the solution methods, has many advantages such as good stoichiometric control and the production of active submicron-size particles in a relatively shorter processing time at a somewhat lower temperature, as compared with that manufactured by the conventional solid-state reaction method.

In rechargeable lithium battery systems, the discharge–charge reaction involves the lithium intercalation into and de-intercalation from the cathode materials. Since the intercalation kinetics at a porous lithium intercalation oxide electrode are generally controlled by the diffusion of lithium ions in the oxide, the determination of the change

* Corresponding author. Tel: +82-42-869-3319; fax: +82-42-869-3310; e-mail: sipyun@sorak.kaist.ac.kr.

0378-7753/98/$19.00

in diffusivity in the oxide with lithium content should provide a better understanding of the lithium intercalation into the oxide electrode.

The present work is concerned with the electrochemical lithium intercalation behavior of porous $LiNiO_2$ electrodes prepared by the conventional solid-state reaction and by sol–gel methods in 1 M $LiPF_6$–EC(ethylene carbonate)/DEC(diethyl carbonate) solution. For this purpose, the two types of $LiNiO_2$ electrode specimens have been prepared and characterized by using X-ray diffractometry (XRD) and a galvanostatic intermittent charge–discharge experiment combined with electrochemical impedance spectroscopy (EIS). The chemical diffusivity of lithium ions in the both electrode specimens was determined as a function of the lithium content $(1-\delta)$ by the analysis of the impedance spectra and is discussed in terms of the cation-mixing effect. In addition, the performance of a cell, Li/organic electrolyte/$LiNiO_2$ electrode prepared by the sol–gel method, is evaluated from the results of a charge–discharge cycling test.

2. Experimental

To prepare the ternary oxide $LiNiO_2$ powders by the sol–gel method, a solution of lithium hydroxide($LiOH \cdot H_2O$) and ammonium hydroxide(NH_4OH) was added to a nickel nitrate($Ni(NO_3)_2$) solution in a molar ratio of metallic ions, Li^+/Ni^{2+}, of 4:1, i.e., 3 molar of lithium is in excess. After a gelatinous precipitate was obtained, the solvents were evaporated off by heating the sol at 90°C and the powder was washed with distilled water for 2 h to remove unreacted lithium compounds. Then, the resulting powder was dried at 120°C for 24 h. Finally, the gel-derived $LiNiO_2$ powder was obtained by heating the dried gelatinous oxide powder in air for 6 h in the temperature range 400 to 600°C. For comparison, a second $LiNiO_2$ powder was prepared by a conventional method that was based on the solid-state reaction of $LiOH \cdot H_2O$ and $Ni(OH)_2$ at 600°C for 6 h in air, followed by heating at 700°C for 12 h in air, with intermittent grinding. The resulting product was ground to below 10 μm in particle size by ball milling. The crystal structures of the two kinds of $LiNiO_2$ powders were characterized by XRD. The powder XRD patterns were recorded on an automated Rigaku diffractometer using Cu Kα radiation.

The two kinds of $LiNiO_2$ electrode specimens were prepared by mixing $LiNiO_2$ powder with 6 wt.% Vulcan XC-72 carbon black and 3 wt.% PVDF(poly-vinylidene fluoride) in NMP(*n*-methyl pyrrolidone) solution. The stirred mixture was spread on 316 stainless-steel ex-met. After evaporation of the NMP, the electrode specimens were dried under vacuum for over 24 h.

A three-electrode electrochemical cell was employed for the electrochemical measurements. The reference electrode, as well as the counter electrode, was constructed from lithium foil (Foote Mineral USA, purity 99.9%), and a 1 M lithium hexafluorophosphate($LiPF_6$) was taken as a lithium salt and the mixture of 50 vol% ethylene carbonate(EC) and 50 vol% diethyl carbonate(DEC) was used as a solvent. The EC and the DEC were dried for at least 24 h with previously activated 5 A molecular sieves and the $LiPF_6$ was dried under vacuum at 90°C for 12 h. The materials were then mixed together.

Galvanostatic intermittent charge–discharge curves were obtained under constant-current conditions by using an EG&G PARC Model 283 potentiostat/galvanostat. The charge and discharge currents were selected so that a change in the lithium content of $\Delta\delta = 1$ for $Li_{1-\delta}NiO_2$ would occur in 2 h. For the electrochemical impedance measurements, a Solartron 1255 Frequency Response Analyser was used in conjunction with the Solartron 1286 Electrochemical Interface under remote control by an IBM compatible personal computer. After the electrode attained an equilibrium potential, the electrochemical impedance measurements were carried out by applying an AC-amplitude of 5 mV_{rms} on an equilibrium electrode potential of 3.2 to 4.2 V_{Li/Li^+} over the frequency range from 1 mHz to 100 kHz. The frequency was scanned from high to low values. The charge–discharge cycling experiment was carried out galvanostatically at constant charge and discharge current densities of 0.5 and 1 mA cm^{-2}, respectively, by using a Bright Model HRC 6064A battery testing unit. All the electrochemical experiments were conducted at room temperature in a glove box (VAC HE493) filled with purified argon gas.

3. Results and discussion

3.1. XRD characterization of synthesized $LiNiO_2$

Fig. 1a–c shows the XRD patterns obtained from gelatinous $LiNiO_2$ powder heat-treated in air for 6 h at 400, 500 and 600°C, respectively. The results of XRD combined with differential scanning calorimetry showed that the crystalline phase proves to be stable at temperatures above 400°C. In $LiNiO_2$ with a layered structure, alternate layers of Li and Ni occupy the octahedral sites of a cubic close packing of oxygen ions. This gives a rhombohedral structure with an $R\bar{3}m$ space group, Li in 3(a), Ni in 3(b) and O in 6(c) sites. The compound shows structural and compositional varieties depending on its conditions of synthesis. It is difficult to obtain the stoichiometric composition of $LiNiO_2$ because the composition decomposes readily to $Li_{1-x}Ni_{1+x}O_2$ at high temperature due to the higher vapour pressure of lithium salts such as LiOH and $LiNO_3$. The new compound can be formulated as $[Li_{1-x}Ni_x]_{3(b)}[Ni]_{3(a)}[O_2]_{6(c)}$ in which the cations of Li^+ and Ni^{3+} are partially mixed between octahedral 3(a) and 3(b) sites [14]. A specimen with a lower x is required in order to realize a higher reversible capacity, because the

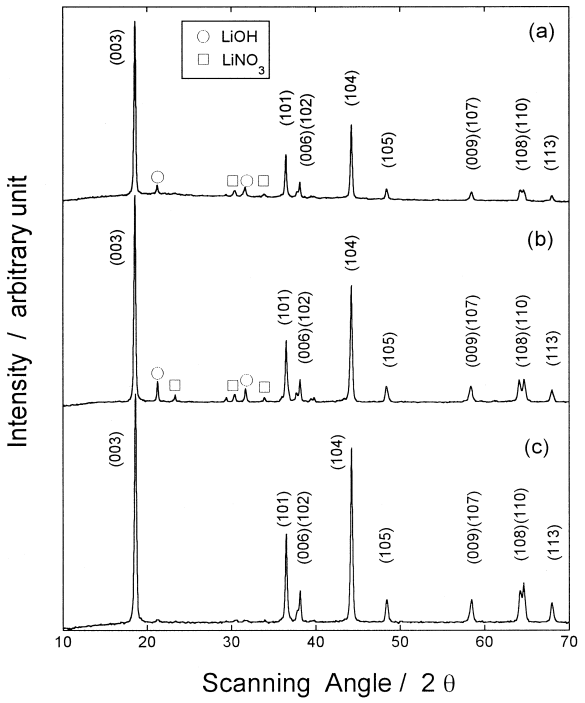

Fig. 1. X-ray diffraction patterns of $LiNiO_2$ powders prepared by sol–gel method at various temperatures : (a) 400°C; (b) 500°C; (c) 600°C. The Miller indices of the Bragg peaks are indicated over each peak.

Ni^{3+} ions substituting Li^+ ion sites are expected to disturb the lithium-ion diffusion. The lithium deficiency is compensated by adding excess lithium salt.

The XRD patterns of 400°C and 500°C heat-treated powder specimens (Fig. 1a and b) are comprised of many sharp crystalline peaks of $LiNiO_2$ and a few small peaks of unreacted lithium compounds (viz., LiOH and $LiNO_3$). A single phase of $LiNiO_2$ was formed when the gelatinous oxide powder was heated at 600°C (Fig. 1c).

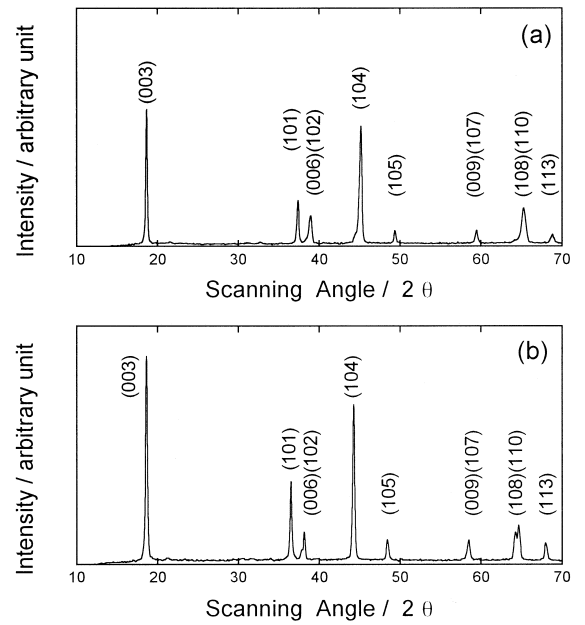

Fig. 2. X-ray diffraction patterns of $LiNiO_2$ powders prepared by (a) solid-state reaction method and (b) sol–gel method. The Miller indices of the Bragg peaks are indicated over each peak.

Fig. 2a and b present XRD patterns of $LiNiO_2$ powders obtained from the conventional solid-state reaction method at 700°C for 12 h and the sol–gel method at 600°C for 6 h, respectively. All diffraction peaks can be indexed by assuming the structure to be a hexagonal lattice of the α-$NaFeO_2$ type and give the lattice parameters $a = 2.886$ Å, $c = 14.214$ Å for the conventional $LiNiO_2$ powder and $a = 2.879$ Å, $c = 14.195$ Å for the gel-derived $LiNiO_2$ powder. The ideal layered $LiNiO_2$ structure has a close-packed oxygen array which is slightly distorted from ideal cubic close packing. The trivalent nickel ions are surrounded by six oxygen atoms and form NiO_2 infinite slabs by edge-sharing of the NiO_6 octahedra. The Li^+ ions are located between the NiO_2 layers in the octahedral sites. Therefore, the $LiNiO_2$ phase has a rhombohedral structure with a space group $R\bar{3}m$ and the unit cell parameters are usually defined in terms of the hexagonal setting [6].

In the case of $LiNiO_2$ or cobalt-substituted phases, special attention has to be drawn to the existence of Ni^{3+} ions present in the Li^+ layers that impede the diffusion of lithium ions. The changes in layer occupancy have a direct effect on the X-ray intensity ratios such as the $I(003)/I(104)$ and $I(006, 102)/I(101)$ ratios [7]. When the integrated intensity ratio of the (003) to (104) peaks falls below 1.2, either the (108) and (110) peaks or the (006) and (102) peaks are scarcely distinguishable from each other. The disordering nature, which is called cation-mixing, can seriously degrade the electrochemical performance of the electrode, such as the rechargeable capacity and the resistance for the electrochemical intercalation reaction. As shown in Fig. 2, it is expected that the electrochemical reactivity of the conventional $LiNiO_2$ powder in comparison with that of the gel-derived powder is poor due to the partial cation-mixing in that electrode. This result strongly suggests that the sol–gel preparation method requires a relatively lower heat-treatment temperature and a shorter heat-treatment time than the solid-state reaction method that needs a temperature above 700°C for more than 12 h. A more homogeneous random mixing of the cations and a less tendency for segregation during the heat treatment are characteristic of the sol–gel method compared with the solid-state reaction method. Thereby, the gel-derived, fine, homogeneous powder mixture makes it possible to form a single phase of the composition $LiNiO_2$.

3.2. Electrochemical characterization by a galvanostatic intermittent charge–discharge experiment

Fig. 3a and b demonstrate the first galvanostatic intermittent charge and discharge curves obtained from the conventional and gel-derived porous $Li_{1-\delta}NiO_2$ elec-

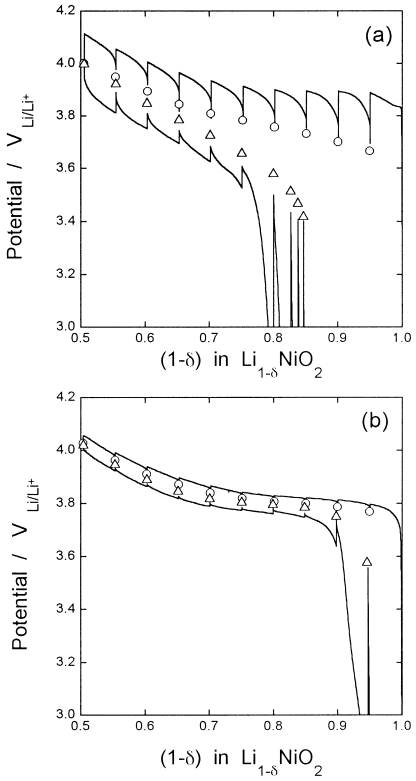

Fig. 3. First galvanostatic intermittent charge–discharge curves of the porous $Li_{1-\delta}NiO_2$ electrodes prepared by (a) solid-state reaction method and (b) sol–gel method in 1 M $LiPF_6$–EC/DEC solution.

trodes, respectively, in 1 M $LiPF_6$–EC/DEC solution in the intercalated lithium content, $(1-\delta)$, range of 0.5 to 1.0. Applying a constant current to the cell composed of the porous $Li_{1-\delta}NiO_2$ electrode specimen during 1800 s upon charging, the resulting cell potential transients were recorded by the solid lines in Fig. 3. After interruption of the current pulse, the decay of the open-circuit potential was followed with time until the fluctuation of this potential fell below 0.01 V_{Li/Li^+}. The value was recorded as an electrode potential and is given by the open circles in Fig. 3. The application and interruption of the constant current continued until the lithium content $(1-\delta)$ reached 0.5, after which the measurements were performed in the reverse direction, i.e., discharging, until $(1-\delta)$ attained 1.0. Similar to the charge curve, the resulting cell potential transients and electrode potentials are marked by solid lines and open triangles, respectively, in Fig. 3. The deviation from the ideal stoichiometry of $LiNiO_2$, δ, is calculated from the values of the masses of the oxides and the total electrical charge that is transferred during the whole charge–discharge cycle.

According to the XRD results, a rhombohedral phase and a monoclinic phase are in equilibrium each other in the lithium content range of $(1-\delta)$ 0.75 to 0.90. Therefore, it is expected that the charge–discharge curve yields a potential plateau due to the co-existence of two phases in that range of $(1-\delta)$. The conventional oxide electrode displays a potential slope in Fig. 3a. This indicates that lithium-ion diffusion proceeds in a rhombohedral single phase present in the oxide electrode. By contrast, the gel-derived electrode exhibits a wide potential plateau that appears near 3.85 V_{Li/Li^+} in Fig. 3b. No phase transition in the conventional oxide electrode is traced to the existence of extra Ni^{3+} ions in the Li^+ layers that impedes the lattice distortion as indicated from Fig. 2a.

The instantaneous IR drop, measured as the difference between the cell potential and the electrode potential, remained nearly constant at a small value of 0.05 V_{Li/Li^+} for the gel-derived $Li_{1-\delta}NiO_2$ electrode, irrespective of the lithium content in the range of $0.5 \leq (1-\delta) \leq 0.9$. This indicates that the electrode has a comparatively higher and nearly constant value of ionic conductivity, as well as electronic conductivity, regardless of the lithium content. The higher electrical conductivity of the gel-derived $LiNiO_2$ electrode specimen used in this work, is explained by a smaller particle size($\approx$ 1 to 10 μm) with a more homogeneous size distribution than the conventional oxide electrode specimen. In Fig. 3a, the conventional $Li_{1-\delta}NiO_2$ electrode exhibited a larger capacity loss and a greater instantaneous IR drop during the first intermittent discharge in comparison with the gel-derived electrode.

In general, the potential profile of the discharge curve is ideally flat or in practice slightly steep for the regular single-phase battery systems such as $Li/SOCl_2$ primary and lead/acid secondary batteries. By contrast, it shows a sigmoidal-shaped curve for a rechargeable lithium battery as shown in Fig. 3. Since the intercalated Li^+ ions are distributed over a finite number of sites, the composition dependence of the electrode potential does not obey purely the Nernst equation, but rather follows an expression modified by the well known adsorption isotherm. Lithium intercalation into a host solid with a layered structure, such as TiS_2, $LiNiO_2$ or $LiCoO_2$, is really a quasi-two-dimensional process that takes place in the alternating two-dimensional van der Waals gaps of the host structure. The process closely follows a sorption isotherm analogous to the Langmuir isotherm, that is, the Gibbs energy is determined by the configurational function $(RT/F)\ln((\delta^*)/(1-\delta^*))$ where δ^* is the lattice occupancy fraction. Furthermore, a strong deviation from the modified Nernst equation is expected due to the Li^+–Li^+ ion and Li^+ ion–NiO_2 lattice interactions. A major contribution is the coulombic repulsion between the intercalated Li^+ ions, partially screened by the NiO_2 lattice. Taking only the nearest neighbor interactions into account or using the mean field theory, the additional coulombic repulsion term is expressed as a linear dependence of the relative concentration of the intercalant Li^+ ion δ^*. Thus, the electrode potential E of $Li_{1-\delta}NiO_2$ gives the following expression as a function of δ^* [15],

$$E = E^\circ - \frac{RT}{F}\left[\ln\frac{\delta^*}{1-\delta^*} - k(\delta^* - 0.5)\right] \quad (1)$$

and

$$\delta^* = \frac{\delta - \delta_{min}}{\delta_{max} - \delta_{min}} \quad , \quad \delta_{min} \leq \delta^* \leq \delta_{max} \qquad (2)$$

where: E° is the standard electrode potential at $\delta^* = 0.5$, and the parameter k represents the interaction energy between the intercalated Li^+ ions in the oxide lattice ($k < 0$, attractive interaction; $k > 0$, repulsive interaction).

In the derivation of Eq. (1), it is assumed that the lattice parameters are invariant during the intercalation reaction, and so the interaction between the Li^+ ion and the NiO_2 lattice is independent of the composition. In practice, the host lattice is always a little distorted by the intercalation, and it may be necessary to include an additional term to account for the changes in the Li^+ ion–NiO_2 lattice interactions. The Li^+–Li^+ ion interactions and the entropy term are always repulsive and tend to distribute the Li^+ ions over the available sites. By contrast, the Li^+ ion–NiO_2 interactions may result in condensation of the intercalant Li^+ ions on the one hand and dilution of the Li^+ ions on the other hand. The counterbalanced condensation and dilution would form the Li-rich phase and Li-poor phase, respectively, which are in co-existence. A phase separation of this type would be seen if the energy gained by a cooperative lattice distortion was sufficiently large to overcome the excess electrostatic repulsion between the participating Li^+ ions. As long as the changes in the Li^+ ion–NiO_2 lattice interactions can be approximated by a linear term of δ^*, the expression for the electrode potential will still obey Eq. (1). The latter does not provide information on the individual contributions to the repulsive and attractive interactions, but simply gives the value of the sum of the individual contributions.

When $(1-\delta)$ becomes close to 1, the ionic conductivity decreases rapidly because the number of available sites for lithium-ion diffusion becomes very small. Considering that E goes to $\pm\infty$ as δ^* approaches 1 and 0 in Eq. (1), respectively, this leads to a strong cell polarization. Fig. 3 a and b shows that this polarization occurs at a lower lithium content for the conventional oxide electrode, compared with the gel-derived electrode. The earlier occurrence of the infinite polarization at the former electrode is caused by the existence of extra Ni^{3+} ions in the Li^+ layers in the electrode, which produces a marked fall in δ^*.

3.3. XRD investigation of the variation in lattice parameters with lithium content

The lattice parameters, a and c, of the gel-derived $Li_{1-\delta}NiO_2$ electrode as a function of the intercalated lithium content $(1-\delta)$ are shown in Fig. 4. The lattice parameter a, which is related to the intra-layer metal–metal distance, decreases monotonously with decreasing lithium content as a result of the oxidation of the Ni^{3+} ion to the smaller Ni^{4+} ion as lithium is removed from the structure. By contrast, it is noted that the lattice parameter c, equal to three times the sum of the interlayer spacing and the slab thickness, increases steadily, followed by a slight decrease, as $(1-\delta)$ decreases from 0.75 down to 0.55 and then to below 0.55.

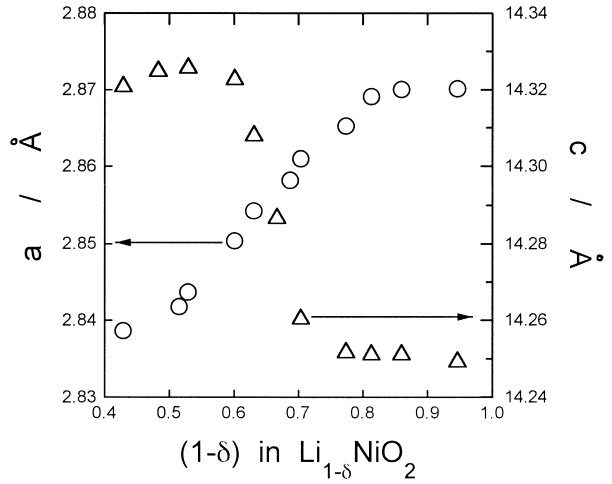

Fig. 4. Hexagonal lattice parameters, a(○) and c(△), of a porous $Li_{1-\delta}NiO_2$ electrode, prepared by the sol–gel method, as a function of lithium content $(1-\delta)$.

Such an increase in the c-direction is the direct result of increasing coulombic repulsions between the negatively charged NiO_2^- layers with the removal of the positively charged Li^+ ion. Since the lattice parameters of $Li_{0.5}NiO_2(R\bar{3}m)$ are very close to those of $LiNiO_2(Fm\bar{3}m)$, which has a rock-salt cubic structure, the cation-mixing occurs easily at $(1-\delta)=0.5$ in $Li_{1-\delta}NiO_2$. In the limiting case, a rock-salt type $LiNiO_2(Fm\bar{3}m)$ appears as a result of 50% cation-mixing of Ni^{3+} and Li^+ ions between their octahedral sites. The presence of Ni^{3+} ions within the van der Waals layer effectively stabilizes the NiO_2^- layers at the low lithium content. Ni^{3+} ions enter the vacant 3(a) octahedral sites by way of diffusion through the adjacent tetrahedral sites that connect the 3(a) and 3(b) octahedral sites of the Ni^{3+} and Li^+ layer, respectively. Therefore, the reversible limit to the lithium de-intercalation from the $Li_{1-\delta}NiO_2$ electrode should be set at $(1-\delta)\approx 0.55$ due to its structural instability, below which the lattice parameter c decreases.

3.4. Electrochemical characterization by impedance spectroscopy

Typical Nyquist plots obtained from the gel-derived $Li_{1-\delta}NiO_2$ electrode in 1 M $LiPF_6$–EC/DEC solution are presented in Fig. 5a. The impedance spectrum consists of two separated arcs in the high- and intermediate-frequency range 50 mHz to 100 kHz, a line inclined at constant angle to the real axis in the low-frequency range 10 mHz to 50

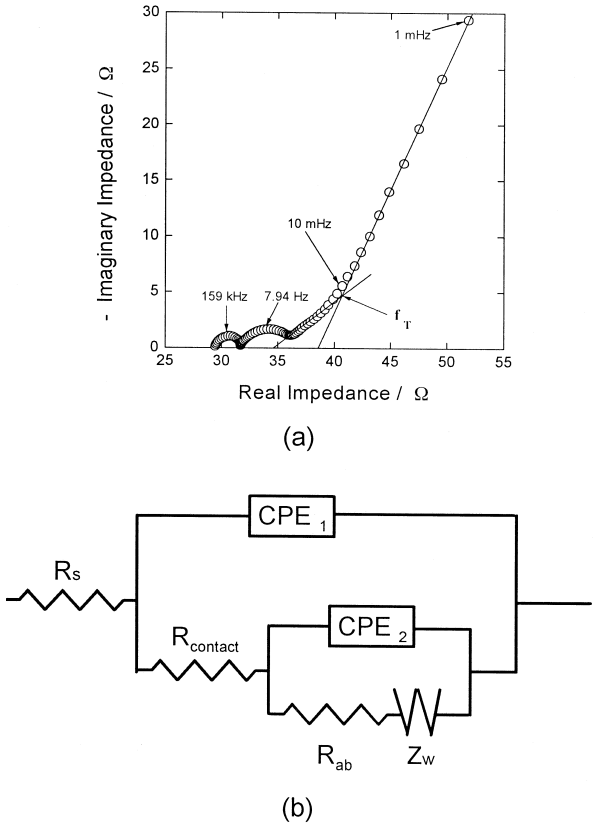

Fig. 5. (a) Typical Nyquist plot obtained from a porous $Li_{1-\delta}NiO_2$ electrode prepared by the sol–gel method in 1 M $LiPF_6$–EC/DEC solution. (b) Equivalent circuit used for analysis of the electrochemical lithium intercalation reaction into a porous $Li_{1-\delta}NiO_2$ electrode in 1 M $LiPF_6$–EC/DEC solution. CPE_i: $A_i(j\omega)_i^n$ where $A_i = R_i^{n_i}\ C_i^{n_i-1}$ with $0.5 < n_i < 1$, $R_i = R_{contact}$ or R_{ab} and $C_i = C_{contact}$ or C_{ad}.

mHz, and a capacitive line due to the accumulation of the Li^+ at the center of the oxide particle in the frequency range below 10 mHz. The two arcs in the higher frequency range are due to the reactions at the interface of the electrolyte/oxide electrode, and the inclined line in the lower frequency range is attributable to a Warburg impedance that is associated with the lithium-ion diffusion in the oxide electrode.

According to the results of previous work [16], the high-frequency arc in the electrode represents the particle-to-particle contract resistance and capacitance among the oxide particles. The high-frequency arc is severely depressed as a result of the porous and inhomogeneous character of the oxide electrode [17]. The degree of depression of the high-frequency arc is found to be 0.72 ~ 0.81 by using the parallel combination of a resistor and a constant phase element (CPE). The impedance of the CPE is defined as:

$$\mathrm{CPE} = B(j\omega)^n,\ j = \sqrt{-1} \tag{3}$$

where: ω is the angular frequency; B and n are constants. When n is -1, CPE becomes an ideal capacitor. Based upon the Conway model [18], the intermediate-frequency arc in the Nyquist plot is related closely to the absorption into the oxide of the Li^+ ions that are adsorbed on the oxide surface.

Based on the Nyquist plot, an equivalent circuit is proposed for the electrochemical lithium intercalation reaction into the porous $Li_{1-\delta}NiO_2$ electrode. This is illustrated in Fig. 5b. Here: R_s represents the sum of the electrolyte and conducting substrate resistances; $R_{contact}$ is the resistance associated with the particle-to-particle contact among the oxide particles; $C_{contact}$, is the contact capacitance due to the accumulation of charged species at the surface of oxide particles; R_{ab}, is the resistance associated with the absorption reaction of adsorbed lithium into the oxide; C_{ad}, is the capacitance arising from the adsorption of lithium in the near-surface region of the oxide; Z_w is the finite length Warburg impedance for the diffusion of lithium ion through the oxide.

3.5. Variation of chemical diffusivity with lithium content by analysis of impedance spectroscopy

The value of the apparent chemical diffusivity $\tilde{D}_{Li^+}$ of lithium ions in the porous $Li_{1-\delta}NiO_2$ electrode has been calculated by using the relation reported by Cabanel et al. [19], i.e.,

$$\tilde{D}_{Li^+} \frac{\pi f_T r^2}{1.94} \tag{4}$$

where f_T is the frequency at which the impedance spectrum shows a transition from semi-infinite diffusion behavior to finite-length diffusion behavior. The value of f_T is determined from Fig. 5a. The average radius r of the oxide particle is derived from scanning electron microscopic observations.

The calculated chemical diffusivities of lithium ions in the conventional and gel-derived oxide electrodes are plotted in Fig. 6a against the lithium content in the range $(1-\delta) = 0.5$ to 0.7. The chemical diffusivities are found to be of the order of 10^{-7} to 10^{-9} $cm^2\ s^{-1}$ at room temperature and the value for both electrodes decreased slightly with lithium content. According to previous work [16], the diffusion of lithium ions through $Li_{1-\delta}NiO_2$ is not influenced by the change of lattice parameter, but rather by the number of vacant sites that are available for Li^+ ions within the Li^+ ion layer. Therefore, the larger chemical diffusivity in the gel-derived oxide electrode than that in the conventional electrode is attributable to the reduced effect of cation-mixing between Ni^{3+} ions and Li^+ ions in the latter electrode.

Considering the thermodynamic enhancement factors obtained from the titration curves in Fig. 3, the component

diffusivities of lithium ion, $D_{Li^+,k}$, in the electrodes are calculated from Eq. (5) [20], i.e.,

$$D_{Li^+,k} = -\frac{RT}{(1-\delta)F}\left(\frac{\partial\delta^*}{\partial E}\right)\tilde{D}_{Li^+} \quad (5)$$

where $-(RT)/((1-\delta)F)((\partial\delta^*)/\partial E))\tilde{D}_{Li^+}$ is the inverse of the thermodynamic enhancement factor. The component diffusivity $D_{Li^+,k}$ is a measure of the random motion of neutral lithium atoms in the absence of a concentration gradient and is mainly determined by the number of vacant sites available for the Li^+ ions in the oxide and the structural modification of the oxide lattice induced by the intercalated Li^+ ions [21]. The calculated component diffusivities of lithium ions in the electrodes as a function of lithium content in the range $(1-\delta) = 0.5$ to 0.7 are given in Fig. 6b. The component diffusivities of the lithium ions in both the electrodes have a nearly constant value of approximately 10^{-11} cm^2 s^{-1} at room temperature, irrespective of the lithium content over the whole range.

3.6. Performance of a cell consisting of: Li / 1 M $LiPF_6$–EC / DEC solution / gel-derived porous $LiNiO_2$ electrode

Fig. 7 presents the variation of specific discharge capacity with the number of cycles for the cell: Li/1 M $LiPF_6$–EC/DEC solution/porous $LiNiO_2$ electrode prepared by the sol–gel method. The stacking pressure of the tightly fitting jelly roll electrode sheets is effective in enhancing the cycle life of a cell with a lithium metal anode. This is because the pressure flattens the morphology of the lithium metal and improves the utilization of the lithium metal anode initially placed in the cell [22]. There is, however, a gradual increase in pressure even for the cell with the tightly fitting jelly roll electrode used this work as the cycle number is increased. This is due to swelling of the deposited Li at each charge stage.

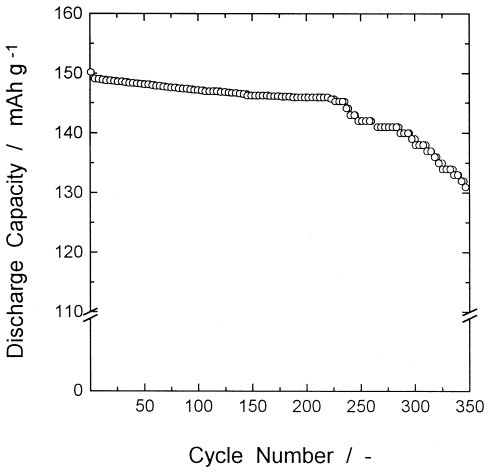

Fig. 7. Variation of specific discharge capacity with cycling for the cell: Li/1 M $LiPF_6$–EC/DEC solution/porous $Li_{1-\delta}NiO_2$ electrode prepared by sol–gel method. The cycling is carried out galvanostatically at constant charge and discharge current densities of 0.5 mA cm^{-2} and 1 mA cm^{-2}, respectively, and between 4.1 and 3.0 V_{Li/Li^+}.

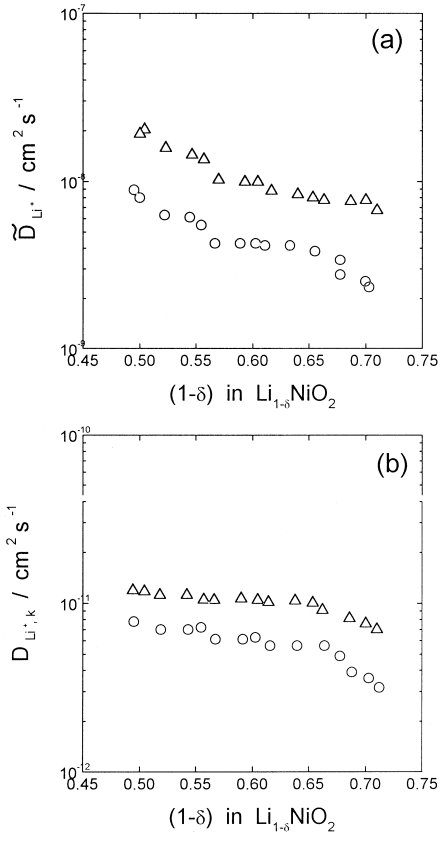

Fig. 6. (a) Chemical diffusivity, $\tilde{D}^+_{Li}$, and (b) component diffusivity, $D^+_{Li,k}$, of lithium ions in porous $Li_{1-\delta}NiO_2$ electrodes prepared by the solid-state reaction method (○) and the sol–gel method (Δ) as a function of lithium content, $(1-\delta)$, at room temperature.

The discharge capacity decreases initially and levels off at approximately 0.55 Li per formula-unit $LiNiO_2$. After 350 cycles, about 90% of the initial capacity can be recovered and gives the gel-derived electrode material a promising specific energy density of above 500 Wh kg^{-1}. Also, the initial specific capacity of 150 Ah kg^{-1} makes this gel-derived oxide material very attractive as a cathode material for rechargeable lithium battery systems.

4. Conclusions

The present work is concerned with studies of the electrochemical lithium intercalation behavior of conventional and gel-derived porous $LiNiO_2$ electrodes in 1 M $LiPF_6$–EC/DEC solution for rechargeable battery systems by using XRD, a galvanostatic intermittent charge–discharge experiment, EIS and a charge–discharge cycling test. From the experimental results, the following conclusions are drawn, as follows.

1. The deviation from the reversibility of the intercalation, as well as the instantaneous IR drop, are larger in a conventional oxide electrode than in a gel-derived elec-

trode. The increased resistance and lowered reversibility for intercalation can be attributed to the enhanced effect of cation-mixing between the Ni^{3+} and Li^{+} ions in the former electrode. This conclusion is supported by XRD data.

2. The chemical diffusivity, which is a rate-determining factor for lithium intercalation, is found to be of the order of 10^{-7} to 10^{-9} cm^2 s^{-1} at room temperature. The value for both electrodes decreases slightly with lithium content. The greater chemical diffusivity in the gel-derived oxide electrode is due to a reduced effect of cation-mixing between the Ni^{3+} and Li^{+} ions.

3. The discharge capacity of a $LiNiO_2$ electrode prepared by the sol–gel method is maintained at above 90% of the initial value for 350 cycles. An initial specific capacity of 150 Ah kg^{-1} and a specific energy density above 500 Wh kg^{-1} for a cell comprised of Li/1 M $LiPF_6$–EC/DEC solution/$LiNiO_2$ electrode suggests that the gel-derived oxide electrode is very attractive as a cathode material for rechargeable lithium battery systems.

Acknowledgements

The receipt of research grant under the programme ‘Development of technology of high performance batteries for electric vehicle application 1996/1997’ from the Ministry of Commerce and Industry, Korea is gratefully acknowledged. Incidentally, the Ministry of Information and Communication, Korea, financially supported this work under the university foundation research programme ‘Development of High Performance Rechargeable Lithium Battery for Telecommunication Application 1996/1997’.

References

[1] M.S. Whittingham, J. Electrochem. Soc. 123 (1976) 315.
[2] S. Atlung, K. West, T. Jacobsen, J. Electrochem. Soc. 126 (1979) 1311.
[3] D.W. Murphy, P.A. Christian, Science 205 (1979) 651.
[4] M. Lazzari, B. Scrosati, J. Electrochem. Soc. 127 (1980) 773.
[5] J.R. Dahn, U. von Sacken, M.W. Juzkow, H. Al-Janaby, J. Electrochem. Soc. 138 (1991) 2207.
[6] J.R. Dahn, U. von Sacken, C.A. Michal, Solid State Ionics 44 (1990) 87.
[7] T. Ohzuku, A. Ueda, M. Nagayama, Y. Iwakoshi, H. Komori, Electrochim. Acta 38 (1993) 1159.
[8] K. Mizushima, P.C. Jones, P.J. Wiseman, J.B. Goodenough, Mat. Res. Bull. 15 (1980) 783.
[9] M.G.S.R. Thomas, P.G. Bruce, J.B. Goodenough, J. Electrochem. Soc. 132 (1985) 1521.
[10] W. Ebner, D. Fouchard, L. Xie, Solid State Ionics 69 (1994) 238.
[11] J. Livage, M. Henry, C. Sanchez, Prog. Solid State Chem. 18 (1988) 259.
[12] J.P. Pereira-Ramos, R. Baddour, S. Bach, N. Baffier, Solid State Ionics 53 (1992) 701.
[13] Q. Lin, T. Yixiong, M. Xuezhang, Q Ruizhen, W Jigiang, J. Power Sources 43 (1993) 309.
[14] H. Arai, S. Okada, H. Ohtsuka, M. Ichimura, J. Yamaki, Solid State Ionics 80 (1995) 261.
[15] M.B. Armand, in: D.W. Murphy, J. Broadhead, B.C.H. Steele (Eds.), Materials for Advanced Batteries, Plenum, New York, 1980, p. 145.
[16] Y.-M. Choi, S.-I. Pyun, J.-S. Bae, S.-I. Moon, J. Power Sources 56 (1995) 25.
[17] R. de Levie, Electrochim. Acta 9 (1964) 1231.
[18] B.E. Conway, J. Electrochem. Soc. 138 (1991) 1569.
[19] R. Cabanel, G. Barral, J.-P. Diard, B. Le Gorrec, C. Montella, J. Appl. Electrochem. 23 (1993) 93.
[20] W. Weppner, R.A. Huggins, J. Electrochem. Soc. 124 (1977) 1569.
[21] Y.-M. Choi, S.-I. Pyun, S.-I. Moon, Solid State Ionics 89 (1996) 43.
[22] T. Hirai, I. Yoshimatsu, J. Yamaki, J. Electrochem. Soc. 141 (1994) 2300.